PRECODING DESIGN FOR THE MIMO-ROC DOWNLINK

Valentina Rizzello[◇,⋆], *Michael Joham*[⋆], *Andrea Matera*[◇], *Wolfgang Utschick*[⋆], *Umberto Spagnolini*[◇]

[⋆]Institute for Signal Processing, Technische Universität München, 80333 München
{valentina.rizzello, joham, utschick}@tum.de
[◇]Dipartimento di Elettronica, Informazione e Bioingegneria (DEIB), Politecnico di Milano, 20133 Milano
{valentina.rizzello, andrea.matera, umberto.spagnolini}@polimi.it

ABSTRACT

MIMO Radio-over-Copper (MIMO-RoC) is a transport system for indoor coverage that leverages the pre-existing building's copper cabling infrastructure. In MIMO-RoC, the overall channel from the Base Band Units (BBU) to the end-user is the cascade of a MIMO-radio over a MIMO-cable channel and the analog fronthaul together with a wireless channel enables the transport to the mobile users. The entire system poses two main challenges: *i)* design low-complexity and flexible allocation strategies between wired and wireless resources; *ii)* design interference cancellation techniques tailored to the mutually coupled wired-wireless interference. While the former has been extensively investigated, the optimal design of precoding algorithms for the MIMO-RoC downlink is still an open issue and is covered here. In particular, in this paper, the Linear Successive Allocation (LISA) algorithm has been revised and adapted to the MIMO amplify-and-forward (AF) structure of MIMO-RoC. Numerical results validate the proposed method considering a realistic radio environment with 100m copper cable remotization.

Index Terms— MIMO, Radio Over Copper, C-RAN, LISA, Zero-forcing precoding

1. INTRODUCTION

With the next generation (5G and beyond) wireless communication systems, new physical layer technologies are required to guarantee high-rate/low-latency connectivity to all the interconnected smart devices [1]. Centralized Radio Access Network (C-RAN) architecture enables the deployment of a massive number of antennas which is an effective solution for both providing high data rate and coping with the high mobile traffic demand [2]. The Remote Antenna Units (RAU) are separated from the BBU that are possibly aggregated to form a BBU pool for centralized processing [3]. In contrast to a digital fronthaul (FH) architecture, in analog FH, the RAUs relay intermediate frequency signals to/from BBUs avoiding any bandwidth expansion due to digitalization or latency, and enabling a more accurate bit/carrier-frequency synchronization. In this scenario, MIMO Radio-over-Copper (MIMO-RoC) represents, an alternative/complementary solution for the last 100–200 m fronthaul (FH) links between multiple RAU and BBU.

The reuse of copper lines for the deployment of femtocells based on amplify-and-forward devices has been proposed in [4]. In [5], a system with remote radio heads (RRH) and shared baseband processors has been presented as solution to achieve full coordination between the small cells and the macro layer, eliminating the main drawback of femtocells. Following on this progress, [6] and [7] explore the case when the radio systems are deployed in coexistence with DSL.

Furthermore, the effectiveness of MIMO-RoC based on LAN cables has been recently proved for both target wireless bandwidth [8] and deployment costs, as each RAU is remotely powered over the same copper cables [9]. However, cables are affected by Insertion Loss (IL) and Far-End-Cross talk (FEXT) that should be properly handled to avoid cable induced degradation, especially at the highest cable frequencies [8], [10]. The issue of crosstalk mitigation in RoC-based systems is covered in [11] and [12] for an LTE-over-Copper architecture. However, the analysis here is limited to low cable frequency, for which IL and FEXT are mild. In contrast, in the considered MIMO-RoC architecture, the cable frequency is pushed up to hundreds of MHz, thus requiring advanced interference cancellation techniques. In particular, the solution to this problem requires *i)* a fair allocation between wireless and wired resources in order to make FEXT and IL effects negligible for the wireless links, and *ii)* efficient algorithms for the precoder design in order to optimize some performance metrics for the wireless link, i.e., the sum rate of the system or the minimum user rate. While for *i)* exist some relevant results referred to as Space-Frequency to Space-Frequency (SF2SF) multiplexing for MIMO RoC [13], [14], [15], the latter problem *ii)* is still open and it is the topic of this paper. In particular, focus here is to design the optimal precoder for the MIMO-RoC downlink, constraining the power jointly for cable and wireless links. In detail: per-line constraints at the cable input and per-antenna constraints at RAU output. Double constraints are fulfilled by adapting the Linear Successive Allocation (LISA) algorithm [16] as computationally simple solution in total-power constrained problems. Moreover, we will show that LISA has a performance similar to that of the optimal zero-forcing based on generalized inverses [17]. After context presentation and model definition, Sect. 3 adapts the LISA problem at hand. More specifically, LISA is adapted for the MIMO-RoC system in order to find the optimal precoder at the BBU, by assuming the amplification at the RAU to be known. Then, we also optimize the amplifier at the RAU and integrate its optimization together with the proposed LISA. We highlight here, that due to the specificity of the system we consider in this work, the RAU has to be modeled as diagonal matrix and not as a full matrix. This makes the amplify-and-forward (AF) optimization different from the ones explored in previous works ([18], [19], [20], [21], [22], [23], [24]). Finally, numerical results validate the presented algorithms.
In this work we assume full CSI knowledge at the receiver, as precoding techniques under imperfect CSI are beyond the scope of the paper.

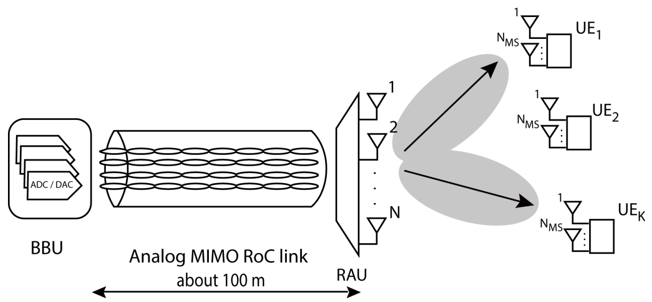

Fig. 1. MIMO-RoC Scenario.

2. SYSTEM MODEL

We consider a C-RAN architecture based on the RoC model operated in the downlink. The signals are transmitted from the BBU to the N RAU over N cables represented by $\boldsymbol{H}_{\text{c}} \in \mathbb{C}^{N\times N}$. The RAU amplify and forward (AF) and use their N antennas to transmit the signals to the K users (see Fig. 1). The RAU work autonomous leading to the diagonal gain matrix $\boldsymbol{F} \in \mathbb{R}^{N\times N}$. With the transmitted signal $\boldsymbol{x}_{\text{c}} \in \mathbb{C}^{N}$, the signal received by N_{MS} antennas at user k reads as

$$\boldsymbol{y}_k = \boldsymbol{H}_k^{\text{H}} \boldsymbol{F} \left(\boldsymbol{H}_{\text{c}}\boldsymbol{x}_{\text{c}} + \boldsymbol{n}_{\text{c}}\right) + \boldsymbol{n}_k \in \mathbb{C}^{N_{\text{MS}}}$$

where $\boldsymbol{H}_k \in \mathbb{C}^{N\times N_{\text{MS}}}$ is the wireless channel from the RAU to user k, $\boldsymbol{n}_{\text{c}} \sim \mathcal{N}_{\mathbb{C}}(\boldsymbol{0}, \sigma_{\text{c}}^2\mathbf{I})$ and $\boldsymbol{n}_k \sim \mathcal{N}_{\mathbb{C}}(\boldsymbol{0}, \mathbf{I})$ denote the noise of the cable channel and the wireless channel of user k, respectively.

In the following, we assume that only $d \leq \min(N, KN_{\text{MS}})$ data symbols are allocated. Therefore, $\boldsymbol{x}_{\text{c}} = \boldsymbol{P}\boldsymbol{t}$ with the data vector $\boldsymbol{t} = [t_1, \ldots, t_d]^{\text{T}} \sim \mathcal{N}_{\mathbb{C}}(\boldsymbol{0}, \mathbf{I})$ and the precoder $\boldsymbol{P} = [\boldsymbol{p}_1, ..., \boldsymbol{p}_d] \in \mathbb{C}^{N\times d}$. Additionally, the columns of $\boldsymbol{P}$ are computed successively. Let $\pi(i)$ be the map from the step index i to the corresponding user. Hence, the output of $\boldsymbol{H}_{\pi(i)}$ is equalized by $\boldsymbol{g}_i \in \mathbb{C}^{N_{\text{MS}}}$ (see Fig. 2; unknown variables optimized here are highlighted in gray).

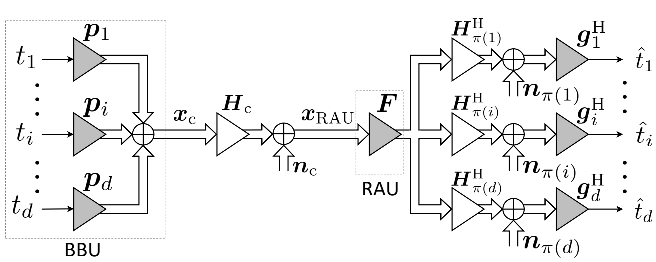

Fig. 2. MIMO-RoC System Model.

3. LISA ALGORITHM FOR MIMO-ROC

In step i, after $i-1$ symbols have been allocated, the Linear Successive Allocation (LISA) algorithm selects the user with the highest SNR and finds the precoder and equalizer pair $\boldsymbol{p}_i$ and $\boldsymbol{g}_i$ jointly. LISA is a zero-forcing scheme suppressing all interference. Therefore, the i-th estimate can be written as

$$\hat{t}_i = \boldsymbol{g}_i^{\text{H}}\boldsymbol{H}_{\pi(i)}^{\text{H}}\boldsymbol{F}\boldsymbol{H}_{\text{c}}\boldsymbol{p}_i t_i + \boldsymbol{g}_i^{\text{H}}\boldsymbol{n}_{\pi(i)} + \boldsymbol{g}_i^{\text{H}}\boldsymbol{H}_{\pi(i)}^{\text{H}}\boldsymbol{F}\boldsymbol{n}_{\text{c}}.$$

Assuming $\boldsymbol{p}_i$ and the index $\pi(i)$ are given, the SNR (and also rate) maximizing equalizer is the matched filter

$$\boldsymbol{g}_i^{\text{H}} = \boldsymbol{p}_i^{\text{H}}\boldsymbol{H}_{\text{c}}^{\text{H}}\boldsymbol{F}\boldsymbol{H}_{\pi(i)}\left(\mathbf{I} + \sigma_{\text{c}}^2\boldsymbol{H}_{\pi(i)}^{\text{H}}\boldsymbol{F}^2\boldsymbol{H}_{\pi(i)}\right)^{-1}. \qquad (1)$$

With above equalizer $\boldsymbol{g}_i$ depending on the precoder $\boldsymbol{p}_i$, the resulting SNR is given by

$$\zeta_i(\boldsymbol{p}_i, \pi(i)) = \boldsymbol{p}_i^{\text{H}}\boldsymbol{H}_{\text{c}}^{\text{H}}\boldsymbol{F}\boldsymbol{H}_{\pi(i)}\boldsymbol{C}_{\text{N},i}^{-1}\boldsymbol{H}_{\pi(i)}^{\text{H}}\boldsymbol{F}\boldsymbol{H}_{\text{c}}\boldsymbol{p}_i.$$

with the noise covariance matrix $\boldsymbol{C}_{\text{N},i} = \mathbf{I} + \sigma_{\text{c}}^2\boldsymbol{H}_{\pi(i)}^{\text{H}}\boldsymbol{F}^2\boldsymbol{H}_{\pi(i)}$. In step i, LISA solves the following optimization problem, i.e., LISA selects the channel with most advantageous SNR,

$$\begin{aligned} \{\boldsymbol{q}_i, \pi(i)\} &= \underset{\{\boldsymbol{q},k\}}{\arg\max}\, \zeta_i(\boldsymbol{q}, k) \\ &\text{s.t.} \quad \boldsymbol{q} \in \text{null}\{\boldsymbol{g}_j^{\text{H}}\boldsymbol{H}_{\pi(j)}^{\text{H}}\boldsymbol{F}\boldsymbol{H}_{\text{c}}\}_{j=1}^{i-1}, \quad \|\boldsymbol{q}\|_2 = 1 \end{aligned} \qquad (2)$$

where $\boldsymbol{q}_i$ is an auxiliary precoding vector that performs partial zero-forcing due to the nullspace constraint. With this constraint, only the interference to already allocated symbols is suppressed. The remaining interference must be suppressed in a second step. Differently from [16], let $\boldsymbol{Q}_i^{\perp} \in \mathbb{C}^{N\times(N-i+1)}$ be the basis for $\text{null}\{\boldsymbol{g}_j^{\text{H}}\boldsymbol{H}_{\pi(j)}^{\text{H}}\boldsymbol{F}\boldsymbol{H}_c\}_{j=1}^{i-1}$ and $\boldsymbol{q}_i = \boldsymbol{Q}_i^{\perp}\boldsymbol{z}_i$ with $\boldsymbol{z}_i \in \mathbb{C}^{(N-i+1)}$. Because of this parametrization, the nullspace constraint can be dropped and the solution $\boldsymbol{z}_i$ is the principal eigenvector of $\boldsymbol{Q}_i^{\perp,\text{H}}\boldsymbol{H}_{\text{c}}^{\text{H}}\boldsymbol{F}\boldsymbol{H}_{\pi(i)}\boldsymbol{C}_{\text{N},i}^{-1}\boldsymbol{H}_{\pi(i)}^{\text{H}}\boldsymbol{F}\boldsymbol{H}_{\text{c}}\boldsymbol{Q}_i^{\perp}$. Note that the parametrization with $\boldsymbol{Q}_i^{\perp}$ reduces computational complexity considerably since $\boldsymbol{z}_i \in \mathbb{C}^{N-i+1}$ instead of $\boldsymbol{q}_i \in \mathbb{C}^{N}$. Moreover, note that $\boldsymbol{Q}_i^{\perp}$ can be efficiently found knowing the householder QR-decomposition of $[\boldsymbol{H}_{\text{c}}^{\text{H}}\boldsymbol{F}\boldsymbol{H}_{\pi(1)}\boldsymbol{g}_1, \ldots, \boldsymbol{H}_{\text{c}}^{\text{H}}\boldsymbol{F}\boldsymbol{H}_{\pi(i-1)}\boldsymbol{g}_{i-1}]$.

3.1. LISA Interference cancellation

Performing (2) successively starting from $i = 1$ and $\boldsymbol{Q}_1^{\perp} = \mathbf{I}$, the auxiliary precoders $\boldsymbol{q}_1, \ldots, \boldsymbol{q}_i$ and the corresponding equalizers $\boldsymbol{g}_1, \ldots, \boldsymbol{g}_i$ can be found.

Using a similar notation as in [16], we define $\boldsymbol{Q}_i = [\boldsymbol{q}_1, ..., \boldsymbol{q}_i]$ and $\boldsymbol{H}_{\text{comp},i} = [\boldsymbol{H}_{\text{c}}^{\text{H}}\boldsymbol{F}\boldsymbol{H}_{\pi(1)}\boldsymbol{g}_1, \ldots, \boldsymbol{H}_{\text{c}}^{\text{H}}\boldsymbol{F}\boldsymbol{H}_{\pi(i)}\boldsymbol{g}_i]^{\text{H}}$ such that $\boldsymbol{H}_{\text{comp},i}\boldsymbol{Q}_i = \boldsymbol{L}_i$ where $\boldsymbol{L}_i$ is a lower triangular matrix due to the nullspace constraint of (2). Then, we cancel the remaining interference by the application of the precoder

$$\boldsymbol{P}_{\text{eff},i} = [\boldsymbol{p}_1, ..., \boldsymbol{p}_i] = \boldsymbol{Q}_i\boldsymbol{L}_i^{-1}\boldsymbol{\Lambda}_i\boldsymbol{\Gamma}_i^{1/2} \qquad (3)$$

where $\boldsymbol{\Lambda}_i = \text{diag}(\lambda_1, \ldots, \lambda_i) = [\text{diag}(\boldsymbol{L}_i^{-1,\text{H}}\boldsymbol{L}_i^{-1})]^{-1/2}$ is a normalization of the columns of $\boldsymbol{Q}_i\boldsymbol{L}_i^{-1}$ to norm one. The power allocation is performed with $\boldsymbol{\Gamma}_i = \text{diag}(\gamma_1, \ldots, \gamma_i)$ where $\gamma_i = \|\boldsymbol{p}_i\|_2^2$.

With all these assumptions, it is guaranteed that the product

$$\boldsymbol{H}_{\text{comp},i}\boldsymbol{P}_{\text{eff},i} = \boldsymbol{\Lambda}_i\boldsymbol{\Gamma}_i^{1/2} \qquad (4)$$

is diagonal and all the interference is suppressed. However, the power constraints at the cable and RAU are left to be fulfilled by the determination of $\boldsymbol{\Gamma}_i$ (as discussed in the next section).

The resulting sum rate reads as [cf. (4)]

$$R_{\text{sum},i} = \log_2\det(\mathbf{I} + \boldsymbol{\Lambda}_i^2\boldsymbol{\Gamma}_i). \qquad (5)$$

The successive algorithm is terminated if $R_{\text{sum},i} < R_{\text{sum},i-1}$ and the number of symbols is $d = i - 1$.

4. POWER ALLOCATION IN SINGLE-CARRIER SCENARIO

In this section, both, the wired and the wireless link, are explored for the single carrier setup.

4.1. Constraints Outline

At the i-th step of LISA, the signal that we transmit through the cable is subject to both the per-line power constraints P_{PL} at the cable input and per-antenna power constraints P_{PA} at the RAU output. These can be reformulated as

$$\begin{aligned}&\forall l = 1, \dots, N:\\ &\left[\boldsymbol{P}_{\text{eff},i}\boldsymbol{P}_{\text{eff},i}^{\text{H}}\right]_{l,l} \leq P_{\text{PL}}, \quad \left[\boldsymbol{H}_{\text{c}}\boldsymbol{P}_{\text{eff},i}\boldsymbol{P}_{\text{eff},i}^{\text{H}}\boldsymbol{H}_{\text{c}}^{\text{H}}\boldsymbol{F}^2\right]_{l,l} \leq P_{\text{PA}}\end{aligned} \tag{6}$$

Here, we assume to have a number of antennas which is equal to the number of twisted pairs in the cable. Moreover, in this analysis, we consider the noise σ_{c}^2 in the cable as negligible compared to the interference.

4.2. Optimization Problem

Recalling the results obtained in Subsection 3.1, we can perform the power allocation such that the diagonal matrix $\boldsymbol{\Gamma}_i$ is the one that maximizes the sum-rate [see (5)]. Therefore, our optimization problem at the i-th step becomes

$$\begin{aligned}&\max_{\boldsymbol{\Gamma}_i \succeq 0} \log_2 \det(\boldsymbol{I} + \boldsymbol{\Lambda}_i^2 \boldsymbol{\Gamma}_i)\\ &\quad\text{s.t.} \quad \left[\boldsymbol{P}_{\text{eff},i}\boldsymbol{P}_{\text{eff},i}^{\text{H}}\right]_{l,l} \leq P_{\text{PL}}\\ &\left[\boldsymbol{F}\boldsymbol{H}_{\text{c}}\boldsymbol{P}_{\text{eff},i}\boldsymbol{P}_{\text{eff},i}^{\text{H}}\boldsymbol{H}_{\text{c}}^{\text{H}}\boldsymbol{F}\right]_{l,l} \leq P_{\text{PA}} \quad \forall l = 1, \dots, N.\end{aligned} \tag{7}$$

4.3. Lagrangian Duality

Since problem (7) is convex, strong duality holds, and we dualize the constraints as

$$\begin{aligned}&\min_{\boldsymbol{\mu}\geq \boldsymbol{0}, \boldsymbol{\nu} \geq \boldsymbol{0}} \max_{\boldsymbol{\Gamma}_i \succeq 0} \log_2 \det(\boldsymbol{I} + \boldsymbol{\Lambda}_i^2 \boldsymbol{\Gamma}_i) - \sum_{l=1}^{N} \mu_l \left[\boldsymbol{P}_{\text{eff},i}\boldsymbol{P}_{\text{eff},i}^{\text{H}}\right]_{l,l}\\ &- \sum_{l=1}^{N} \nu_l \left[\boldsymbol{F}\boldsymbol{H}_{\text{c}}\boldsymbol{P}_{\text{eff},i}\boldsymbol{P}_{\text{eff},i}^{\text{H}}\boldsymbol{H}_{\text{c}}^{\text{H}}\boldsymbol{F}\right]_{l,l} + \sum_{l=1}^{N} (\mu_l P_{\text{PL}} + \nu_l P_{\text{PA}}).\end{aligned} \tag{8}$$

By setting $\operatorname{diag}(\boldsymbol{\mu}) = \kappa \operatorname{diag}(\boldsymbol{\mu}') = \kappa \boldsymbol{M}'$ and $\operatorname{diag}(\boldsymbol{\nu}) = \kappa \operatorname{diag}(\boldsymbol{\nu}') = \kappa \boldsymbol{N}'$, where κ is a positive scalar constant, (8) can be rewritten as

$$\begin{aligned}&\min_{\kappa} \min_{\boldsymbol{\mu}'\geq \boldsymbol{0}, \boldsymbol{\nu}' \geq \boldsymbol{0}} \max_{\boldsymbol{\Gamma}_i \succeq 0} \log_2 \det(\boldsymbol{I} + \boldsymbol{\Lambda}_i^2 \boldsymbol{\Gamma}_i) + \kappa P_\kappa\\ &\quad - \kappa \left(\operatorname{tr}\left(\boldsymbol{M}'\boldsymbol{P}_{\text{eff},i}\boldsymbol{P}_{\text{eff},i}^{\text{H}}\right) + \operatorname{tr}\left(\boldsymbol{N}'\boldsymbol{F}\boldsymbol{H}_{\text{c}}\boldsymbol{P}_{\text{eff},i}\boldsymbol{P}_{\text{eff},i}^{\text{H}}\boldsymbol{H}_{\text{c}}^{\text{H}}\boldsymbol{F}\right)\right)\end{aligned} \tag{9}$$

where $\kappa P_\kappa = \sum_{l=1}^{N} (\mu_l P_{\text{PL}} + \nu_l P_{\text{PA}})$.

We define $\boldsymbol{B} = \boldsymbol{H}_{\text{c}}^{\text{H}}\boldsymbol{F}\boldsymbol{N}'\boldsymbol{F}\boldsymbol{H}_{\text{c}} + \boldsymbol{M}'$ and $\boldsymbol{P}_{\text{eff},i} = \boldsymbol{P}_{\text{norm},i}\boldsymbol{\Gamma}_i^{1/2}$. Therefore, (9) simplifies to

$$\begin{aligned}&\min_{\kappa} \min_{\boldsymbol{\mu}'\geq \boldsymbol{0}, \boldsymbol{\nu}' \geq \boldsymbol{0}} \max_{\boldsymbol{\Gamma}_i \succeq 0} \log_2 \det(\boldsymbol{I} + \boldsymbol{\Lambda}_i^2 \boldsymbol{\Gamma}_i) + \kappa P_\kappa\\ &\qquad\qquad - \kappa \left(\operatorname{tr}\left(\boldsymbol{P}_{\text{norm},i}^{\text{H}}\boldsymbol{B}\boldsymbol{P}_{\text{norm},i}\boldsymbol{\Gamma}_i\right)\right).\end{aligned} \tag{10}$$

A further simplification is given by the fact that $\operatorname{tr}(\boldsymbol{C}_i\boldsymbol{\Gamma}_i) = \operatorname{tr}\left(\boldsymbol{P}_{\text{norm},i}^{\text{H}}\boldsymbol{B}\boldsymbol{P}_{\text{norm},i}\boldsymbol{\Gamma}_i\right)$, where $\boldsymbol{C}_i = \operatorname{diag}(\boldsymbol{P}_{\text{norm},i}^{\text{H}}\boldsymbol{B}\boldsymbol{P}_{\text{norm},i})$.

4.4. Dual Problem Solution

By having a closer look at (10), we can observe that it is the dual problem of

$$\begin{aligned}&\min_{\boldsymbol{\mu}'\geq \boldsymbol{0}, \boldsymbol{\nu}' \geq \boldsymbol{0}} \max_{\boldsymbol{\Gamma}_i \succeq 0} \log_2 \det(\boldsymbol{I} + \boldsymbol{\Lambda}_i^2 \boldsymbol{\Gamma}_i)\\ &\qquad\text{s.t.} \qquad \operatorname{tr}(\boldsymbol{C}_i\boldsymbol{\Gamma}_i) \leq P_\kappa.\end{aligned} \tag{11}$$

By defining $\boldsymbol{\Psi}_i = \boldsymbol{C}_i\boldsymbol{\Gamma}_i$ and $\boldsymbol{\Phi}_i = \boldsymbol{C}_i^{-1}\boldsymbol{\Lambda}_i^2$, we rewrite (11) as

$$\begin{aligned}&\min_{\boldsymbol{\mu}'\geq \boldsymbol{0}, \boldsymbol{\nu}' \geq \boldsymbol{0}} \max_{\boldsymbol{\Psi}_i \succeq 0} \log_2 \det(\boldsymbol{I} + \boldsymbol{\Phi}_i \boldsymbol{\Psi}_i)\\ &\qquad\text{s.t.} \qquad \operatorname{tr}(\boldsymbol{\Psi}_i) \leq P_\kappa.\end{aligned} \tag{12}$$

From (12), it can be noticed that for fixed $\boldsymbol{\mu}'$ and $\boldsymbol{\nu}'$, and therefore for fixed $\boldsymbol{C}_i$, the solution to the inner optimization problem is given by the waterfilling procedure. Hence, what has to be performed is a minimization with respect to $\boldsymbol{\mu}' \geq 0$ and $\boldsymbol{\nu}' \geq 0$ of the waterfilling solution which is a function of the parameters $\boldsymbol{\mu}'$ and $\boldsymbol{\nu}'$. The Lagrangian multipliers $\boldsymbol{\mu}'$ and $\boldsymbol{\nu}'$ can be obtained with the help of a subgradient iteration.

5. RAU OPTIMIZATION

In this section, we focus on the optimization of the diagonal matrix $\boldsymbol{F}$ at the RAU. Let us assume that the LISA stops after having allocated d data symbols (allocating $d+1$ data symbols would decrease the throughput). Therefore, we obtain the optimal $\boldsymbol{P}_{\text{eff},d}$, such that $\boldsymbol{H}_{\text{comp},d}\boldsymbol{P}_{\text{eff},d} = \boldsymbol{D}$, where $\boldsymbol{D} = \boldsymbol{\Lambda}_d\boldsymbol{\Gamma}_d^{1/2}$ is diagonal. Since we want to maximize the throughput, that depends on $\boldsymbol{D}$, we find the optimal $\boldsymbol{F}$ as

$$\begin{aligned}&\max_{\boldsymbol{F},\xi} \xi\\ &\text{s.t.} \quad \Re\left\{\operatorname{tr}\left(\boldsymbol{H}_{\text{eff},d}\boldsymbol{F}\tilde{\boldsymbol{P}}_{\text{eff},d}\right)\right\} \geq \xi \operatorname{tr}(\boldsymbol{D})\\ &\left[\boldsymbol{F}\tilde{\boldsymbol{P}}_{\text{eff},d}\tilde{\boldsymbol{P}}_{\text{eff},d}^{\text{H}}\boldsymbol{F}\right]_{l,l} \leq P_{\text{PA}} \quad \forall l = 1, ...N\end{aligned} \tag{13}$$

where $\tilde{\boldsymbol{P}}_{\text{eff},d} = \boldsymbol{H}_{\text{c}}\boldsymbol{P}_{\text{eff},d}$, and $\boldsymbol{H}_{\text{eff},d} = \left[\boldsymbol{H}_{\pi(1)}\boldsymbol{g}_1, \dots, \boldsymbol{H}_{\pi(d)}\boldsymbol{g}_d\right]^{\text{H}}$ and ξ is an auxiliary scalar. This is a convex optimization problem and can be easily solved. Moreover, by solving the system of KKT conditions it turns out that $\boldsymbol{F}$ has to be real as precisely assumed in the previous sections. However, this new $\boldsymbol{F}$, which is generally not a scaled version of the $\boldsymbol{F}$ used for LISA, destroys the zero-forcing performed before by LISA itself. Therefore, in order to achieve the optimal we have to iterate among LISA and problem (13) until they both converge to the same sum-rate value.

6. NUMERICAL RESULTS

We demonstrate our results using two numerical examples. In the first example, we assume $K = 4$ users with $N_{\text{MS}} = 1$ antenna each, RAU with 4 antennas arranged as a Uniform Rectangular Array (URA), a 100 m LAN cable CAT-6 with $N = 4$ lines. For the wired channel, we exploit a bandwidth that has a carrier frequency centered around 150 MHz (see [8] for IL and FEXT values, [25] and [26] for cable model) and, for the wireless channel, we use the model with a single dominant path affected by Rayleigh fading. We highlight that in this first example, we consider $\boldsymbol{F}$ as a fixed scaled identity matrix. Finally, we use the sum-rate as performance metric. In Fig. 3, the SNR has been defined as SNR = P_{PL} = P_{PA}, and the sum-rate has been averaged over 400 Monte Carlo simulations.

For comparison, we estimate the average throughput of the LISA algorithm described above (diamond markers) against two different algorithms (square markers). First, the solid line represents the case in which throughput has been computed following the zero-forcing based on generalized inverses algorithm [17]. Second, the black dashed line represents the same algorithm [17], but computed only with respect to the users selected by LISA.

The performance of the second version of [17] is apparently better than the first one. LISA chooses the users that are in the best condition and can actually increase the throughput. Moreover, it has been shown that with the same premises, therefore with the same number of users, the performance of LISA, that basically computes a computationally efficient pseudoinverse, are very close to the one of the algorithm in [17]. LISA successively allocates finding local optima, obviously, suboptimal. However, compared to LISA, the latter algorithm requires higher computational effort due to the solution of a Second Order Cone Programming (SOCP) problem and has to be solved with a MAXDET software i.e., [27].

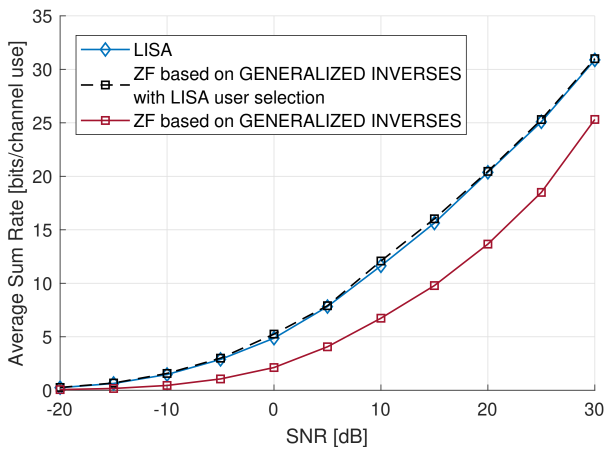

Fig. 3. Average sum rate vs SNR, $N_{\text{MS}} = 1$, $N = 4$, $K = 4$.

In the second example (see Fig. 4), we want to show how the optimization with respect to $\boldsymbol{F}$ improves the average throughput. In this setting, we exploit a cable with 8 twisted pairs at a carrier frequency centered around 50 MHz (see [28] for the interference values), 8 antennas RAU, and 8 users with 2 antennas each. Once again, we use a Rayleigh model for the wireless channel, while the sum-rate has been averaged over 300 Monte Carlo simulations. As in the previous case, we choose a meaningful scaled identity $\boldsymbol{F}$, for comparing our results. As a further analysis in Fig. 5, we compute the user rate dispersion and the average rate per user, where the former is the coloured area between the maximum and the minimum user rate. In particular, we can see how by optimizing $\boldsymbol{F}$, we increase both the maximum and the average rate per user, while guaranteeing the minimum. However, since we are optimizing the sum rate, without taking into account any fairness criteria, we can see that the user rate dispersion is pretty high as expected.

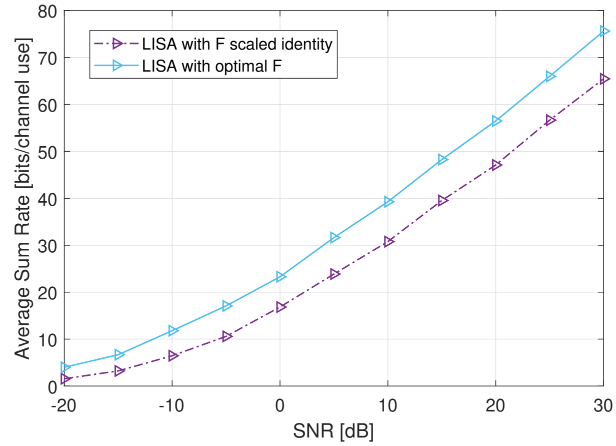

Fig. 4. Average sum rate vs SNR, $N_{\text{MS}} = 2$, $N = 8$, $K = 8$.

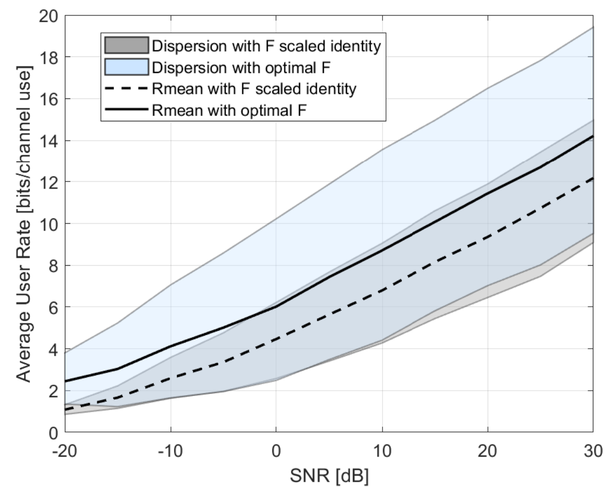

Fig. 5. User Rate Dispersion.

7. CONCLUSION

This paper proposes the optimal downlink precoder design for the MIMO Radio-over-Copper architecture. In MIMO-RoC, the BaseBand Unit (BBU) communicates with multiple users through a multiple-antenna Remote Antenna Unit (RAU) acting as an amplify-and-forward (AF) relay node, and the fronthaul link between BBU and RAU is made by mutually interfering copper-cables. The MIMO-RoC precoder optimization problem is thus complicated by the cascade of MIMO radio and MIMO cable channels, each of which with different constraints to be fulfilled: per-line power constraints at the cable input plus per-antenna power constraints at the RAU antennas. Both constraints are met here by adapting the Linear Successive Allocation (LISA) algorithm to the AF structure of MIMO-RoC. In particular, we first design the optimal LISA-based precoding algorithm to be performed at the BBU by fixing the amplify matrix at the RAU. Then, we also optimize RAU amplification, and its optimization is integrated into the overall precoding design. Numerical results for realistic radio environment and 100m copper cable show that the proposed LISA algorithm for MIMO-RoC attains the performance of optimal zero-forcing with generalized inverses, considered here as performance upper bound. Furthermore, the low complexity of LISA makes the method suitable for real-time implementations.

8. REFERENCES

[1] F. Boccardi, R. W. Heath, A. Lozano, T. L. Marzetta, and P. Popovski, "Five disruptive technology directions for 5G," *IEEE Communications Magazine*, vol. 52, no. 2, pp. 74–80, February 2014.

[2] B. Mahapatra, A. K. Turuk, S. K. Patra, and P. Maiti, "Optimization in fronthaul and backhaul network for cloud RAN (C-RAN): Design and deployment challenges," in *2016 International Conference on Signal Processing, Communication, Power and Embedded System (SCOPES)*, Oct 2016, pp. 1009–1014.

[3] R. Wang, H. Hu, and X. Yang, "Potentials and Challenges of C-RAN Supporting Multi-RATs Toward 5G Mobile Networks," *IEEE Access*, vol. 2, pp. 1187–1195, 2014.

[4] J. Gambini and U. Spagnolini, "Wireless over cable for femtocell systems," *IEEE Communications Magazine*, vol. 51, no. 5, pp. 178–185, May 2013.

[5] E. Trojer P.-E. Eriksson K. Laraqui O.Tridblad C. Lu, M. Berg and H. Almeida, "Connectiong the dots: small cells shape up for high performance indoor radio," *Ericsson Review*, vol. 91, no. 2, pp. 38–45, 2014.

[6] Y. Huang, E. Medeiros, S. Höst, T. Magesacher, P. Eriksson, C. Lu, P. Ödling, and P. O. Börjesson, "Enabling DSL and radio on the same copper pair," in *2015 IEEE International Conference on Communications (ICC)*, June 2015, pp. 1031–1035.

[7] Y. Huang, E. Medeiros, N. Fonseca, S. Höst, T. Magesacher, P. Eriksson, C. Lu, P. Ödling, and P. O. Börjesson, "LTE over copper Potential and limitations," in *2015 IEEE 26th Annual International Symposium on Personal, Indoor, and Mobile Radio Communications (PIMRC)*, Aug 2015, pp. 1339–1343.

[8] S. H. R. Naqvi, A. Matera, L. Combi, and U. Spagnolini, "On the Transport Capability of LAN Cables in All-Analog MIMO-RoC Fronthaul," in *2017 IEEE Wireless Communications and Networking Conference (WCNC)*, 2017, pp. 1–6.

[9] F. Tonini, M. Fiorani, M. Furdek, C. Raffaelli, L. Wosinska, and P. Monti, "Radio and Transport Planning of Centralized Radio Architectures in 5G Indoor Scenarios," *IEEE Journal on Selected Areas in Communications*, vol. 35, no. 8, pp. 1837–1848, Aug 2017.

[10] G. Ginis and J. M. Cioffi, "Vectored transmission for digital subscriber line systems," *IEEE Journal on Selected Areas in Communications*, vol. 20, no. 5, pp. 1085–1104, June 2002.

[11] E. Medeiros, Y. Huang, T. Magesacher, S. Höst, P. Eriksson, C. Lu, P. Ödling, and P. O. Börjesson, "Crosstalk Mitigation for LTE-Over-Copper in Downlink Direction," *IEEE Communications Letters*, vol. 20, no. 7, pp. 1425–1428, July 2016.

[12] Y. Huang, E. Medeiros, T. Magesacher, S. Höst, C. Lu, P. Eriksson, P. Ödling, and P. O. Börjesson, "Time-domain precoding for LTE-over-copper systems," in *2016 IEEE International Conference on Communications (ICC)*, May 2016, pp. 1–6.

[13] A. Matera and U. Spagnolini, "Analog MIMO-RoC Downlink with SF2SF," *IEEE Wireless Communications Letters*, pp. 1–1, 2018.

[14] A. Matera, L. Combi, S. H. R. Naqvi, and U. Spagnolini, "Space-frequency to space-frequency for MIMO radio over copper," in *2017 IEEE International Conference on Communications (ICC)*, May 2017, pp. 1–6.

[15] A. Matera and U. Spagnolini, "On the optimal Space-Frequency to Frequency mapping in indoor single-pair RoC fronthaul," in *2017 European Conference on Networks and Communications (EuCNC)*, June 2017, pp. 1–5.

[16] W. Utschick, C. Stöckle, M. Joham, and J. Luo, "Hybrid LISA Precoding for Multiuser Millimeter-Wave Communications," *IEEE Transactions on Wireless Communications*, vol. 17, no. 2, pp. 752–765, 2018.

[17] A. Wiesel, Y. C. Eldar, and S. Shamai, "Zero-Forcing Precoding and Generalized Inverses," *IEEE Transactions on Signal Processing*, vol. 56, no. 9, pp. 4409–4418, 2008.

[18] A. Liu and V. K. N. Lau and Y. Liu, "Duality and Optimization for Generalized Multi-Hop MIMO Amplify-and-Forward Relay Networks With Linear Constraints," *IEEE Transactions on Signal Processing*, vol. 61, no. 9, pp. 2356–2365, May 2013.

[19] Q. Xiao and M. Dong and B. Liang, "On performance of multi-antenna relay beamforming with per-antenna power constraints," in *2012 Conference Record of the Forty Sixth Asilomar Conference on Signals, Systems and Computers (ASILOMAR)*, Nov 2012, pp. 1371–1375.

[20] F. Tseng and C. Lin and W. Wu, "Optimum Transceiver Designs in Two-Hop Amplify-and-Forward MIMO Relay Systems With SIC Receivers," *IEEE Transactions on Vehicular Technology*, vol. 64, no. 3, pp. 985–997, March 2015.

[21] H. Kong and C. Song and H. Park and I. Lee, "Shaping-Power-Constrained Transceiver Designs for MIMO AF Relaying Systems With Direct Link," *IEEE Transactions on Wireless Communications*, vol. 14, no. 1, pp. 294–304, Jan 2015.

[22] C. Xing and F. Gao and Y. Zhou, "A Framework for Transceiver Designs for Multi-Hop Communications With Covariance Shaping Constraints," *IEEE Transactions on Signal Processing*, vol. 63, no. 15, pp. 3930–3945, Aug 2015.

[23] H. Tang and W. Chen and J. Li, "Robust Joint Source-Relay-Destination Design Under Per-Antenna Power Constraints," *IEEE Transactions on Signal Processing*, vol. 63, no. 10, pp. 2639–2649, May 2015.

[24] L. Sanguinetti and A. A. D'Amico and Y. Rong, "A Tutorial on the Optimization of Amplify-and-Forward MIMO Relay Systems," *IEEE Journal on Selected Areas in Communications*, vol. 30, no. 8, pp. 1331–1346, September 2012.

[25] R. Strobel and R. Stolle and W. Utschick, "Wideband modeling of twisted-pair cables for MIMO applications," in *2013 IEEE Global Communications Conference (GLOBECOM)*, Dec 2013, pp. 2828–2833.

[26] , "IEEE Standard for Ethernet," *IEEE Std 802.3-2015 (Revision of IEEE Std 802.3-2012)*, vol. , no. , pp. 1–4017, March 2016.

[27] Löfberg, J., "YALMIP : A Toolbox for Modeling and Optimization in MATLAB," in *In Proceedings of the CACSD Conference*, Taipei, Taiwan, 2004.

[28] British Telecom, "G.fast: Release of BT cable (100 pair) measurements for use in simulations," *ITU-T SG15 contribution 1422, Geneva, Switzerland*, June 2015.